J. Fluid Mech. (1996), *vol.* 314, *pp.* 27–52

Flow through a perforated surface due to shock-wave impact

By B. W. SKEWS[1] AND K. TAKAYAMA[2]

[1] School of Mechanical Engineering, University of the Witwatersrand, Johannesburg, South Africa
[2] Institute of Fluid Science, Tohoku University, Sendai, Japan

(Received 15 May 1995 and in revised form 17 November 1995)

The factor which is of prime importance in influencing the shock reflection geometry, and resulting pressures, following impingement of a shock wave on a porous surface is the velocity of the flow into the surface. A set of experiments has been conducted, using holographic inferometry in a shock tube, on the impingement of a shock wave on a surface covered with slits, over the full range of shock incidence angles from 0 to 90°. Inverse shock pressure ratios of 0.4, 0.5 and 0.7 were used, and detailed characterization of the flow fields determined. A number of methods are used to infer the inflow into the surface, and measurements are also conducted on the downstream side of the slit plate in order to establish the pressure ratio across the plate. The tests include choking of the flow through the slits. Shock reflection angles are found to be depressed compared to reflection from an impervious wall for cases of regular reflection, but are similar in the case of Mach reflection with the incident wave near glancing incidence. Contrary to assumptions made in previous work it is shown that for wall angles from zero up to approximately 60° the inflow to the plate is inclined to the surface at about 17° and then tends to straighten out until, for normal shock reflection, the flow is also normal to the plate. It appears that this behaviour is linked to the separation of the flow at the inlet to the pores of the model, due to shock wave diffraction. The maximum value of the absolute inflow velocity occurs in the region of transition from regular to Mach reflection. A series of starting vortices is shed on the underside of the slit and is found to follow a path nearly normal to the plate. These vortices lie along a contact surface whose motion is compatible with the strength of the shock wave transmitted through the plate.

1. Introduction

It is becoming increasingly apparent from a number of experimental measurements over the past decade that the properties of a reflecting surface have a significant influence on the reflection geometry of shock waves striking such surfaces, and hence on the pressures that are generated. The effects of surface roughness and the presence of dust layers have been reasonably well characterized (Takayama, Onodera & Gotah 1982; Reichenbach 1985; Ben-Dor *et al.* 1987; Suzuki & Adachi 1987), particularly as they affect the transition from regular to Mach reflection. In general the effect is a reduction in the triple-point trajectory angle resulting in a smaller wedge angle for transition to Mach reflection, ascribed to either viscous (Ben-Dor *et al.* 1987) or inviscid (Reichenbach 1985) effects. In some cases with a dust layer, a second reflected shock appears, the first arising from the top surface of the dust layer and the second from the interface between the dust layer and the supporting wall. Careful experimentation in some of these reports has shown that the process is not pseudo-

stationary, in the sense that triple-point trajectories do not emanate from the leading edge of the wedge although the trajectories are straight lines (Reichenbach 1985). In the case of guttered wedges (Adachi, Kobayashi & Suzuki 1992) it is shown that an additional dimensionless parameter L/x comes into play, where x is a characteristic dimension of the gutter, such as its width, and L is the distance the incident shock wave has moved up the wedge. With large L/x the triple-point trajectory angle approaches that of a smooth wall and the reflection approaches local self-similarity. A short review of the limited data available on interactions with porous surfaces has recently been given by Skews (1995). It is already clear that the effects can be even more marked than for rough surfaces. Besides having application to surfaces covered with porous material, it is also of interest for more complete understanding of blast propagation over permeable soil, snow, and even grasslands or forest.

The reason why experiments on the transition of shock reflection on a smooth wedge show the persistence of regular reflection beyond the theoretically expected limit has been ascribed to the development of a boundary layer on the wall immediately behind the shock (Hornung & Taylor 1982). This is relevant to the present investigation in that, in a frame of reference fixed at the reflection point, the boundary layer has a negative displacement thickness and the effect is thus of a mass inflow into the wall, so that reflected shock waves can exist which do not have to turn the flow parallel to the wall, as required in an idealized inviscid calculation.

Early work conducted on porous surfaces was done predominantly for the case of one-dimensional flow with the shock wave striking the surface normally. Beavers & Matta (1972) investigated the strength of the reflected wave for three different porous materials. Their theoretical model assumed that no shock wave is transmitted into the material and that the flow through the material is steady. An allowance was made for a thin inlet and outlet region, a few pore diameters in extent, where the flow adjusts to the effects of area change, and before frictional effects can have an effect. As will be seen in the present study the effects of a vena-contracta as the flow enters the material can be significant. The flow through the bulk of the material was assumed to follow an extended Darcy equation. The predictions are generally good considering the dramatic assumption of the neglect of transient effects.

In the late 1970s and early 1980s attention was predominantly focused on flows through materials with deformable skeletons (predominantly polyurethane foams) because of the interesting property of pressure amplification if a foam material is positioned against a rigid wall and is struck by a shock wave (Gelfand, Gubonov & Timofeev 1983; Govzdeva *et al.* 1986). These treatments assume the interface between the porous material and the upstream gas to be impervious, with the weakening of the reflected wave being caused by the movement of the interface. In similar tests Skews (1991) presented some evidence of slight inflows for these materials, and suggested that the mechanism for the development of the reflected wave was a combination of wave reflection from the cell walls at the interface, and frictional effects and wave reflections within the body of the material resulting in pressure signals being propagated back out through the interface. These two mechanisms will be discussed further subsequently. The existence of the gas inflow in these one-dimensional cases was subsequently confirmed through numerical studies (Baer 1995) whose model closely predicted the experimental results. Inflows were of the order of 2 m s^{-1} through the interface between the gas and the foam, for an incident shock with a Mach number of 1.4 impacting on a polyurethane foam with a density of 32.5 kg m^{-3}. The interface itself is driven down the shock tube at about 55 m s^{-1}.

One-dimensional studies by van der Grinten, van Dongen & van der Kogel (1985)

using a stiff porous matrix consisting of sand particles bonded together and saturated with air, considerably reduced the effects of skeleton motion which dominate the tests described above. They found that the wave transmitted into the material was fully dispersed with increasing rise time as the wave penetrated further into the material, and that the flow behaviour could be adequately described by a frictional model based on the Forcheimer equation. Levy *et al.* (1993), however, found that by using rigid materials with a much coarser pore structure (e.g. 10 pores per in.) the leading edge of the transmitted wave remained as a shock which decreased in strength as the material was penetrated. The remainder of the wave had the dispersed structure noted by van der Grinten *et al.* (1985). They thus proposed that there were essentially two time (or length) scales operating: a short time scale which controlled the initial reflection process through the reflection, diffraction, and re-reflection of wavelets within the pore structure feeding perturbations back into the external flow thereby strengthening the reflected wave, and a longer time scale phenomenon due to frictional effects as the flow was dominated more and more by the diffusion of viscous effects throughout the matrix. The current study deals with the first of these.

The earliest quantitative two-dimensional study undertaken of shock-wave impact on a perforated surface is that of Friend (1958). A thorough investigation was conducted of the reflection of a shock wave from a perforated plate situated at angles of 45°, 60°, 75° and 90° to the direction of shock motion, all corresponding to regular reflection conditions. Circular holes $\frac{1}{4}$ in. in diameter were drilled over the surface of a $\frac{1}{8}$ in. thick plate with a spacing between holes giving 50% open area. Shock pressure ratios from 2 to 10 in steps of 2 were used, which in all cases but the lowest resulted in the holes choking. The evidence for this was the typical shock diamond pattern of a supersonic jet, downstream of the holes. This feature gave the author the additional boundary condition of sonic conditions at the hole from which to develop his theoretical analysis. Allowance for the vena-contracta was made by using an empirically determined contraction coefficient (referred to as a discharge coefficient), which was found to have a value of about 0.93 for the majority of the tests. Furthermore, because of the relative thinness of the plate he also assumed that the tangential component of velocity is identical on both sides of the plate, i.e. that there is no tangential momentum interchange. These assumptions, together with the use of oblique shock relations, enabled theoretical predictions to be made of the phenomena and these were found to predict the experimental measurements with a fair degree of accuracy. His tests also showed no effect of Reynolds number. The current test boundary conditions are somewhat different from those of Friend, resulting in a wider base of experimental information. Firstly, weaker shocks were chosen so that the holes did not always choke, and secondly the full range of wall angles is investigated so that both regular and Mach reflection occur. Somewhat narrower openings were also used in order to minimize the lack of self-similarity noted above from the work of Adachi *et al.* (1992), typical values of L/x being about 60.

Other early two-dimensional studies were largely aimed at the development of methods for reducing reflected wave strength. Cloutier *et al.* (1971) attempted to attenuate the wave resulting from a 0.303 bullet reflecting off an adjacent surface so that the wave would not interfere with the bullet wake. A variety of materials were tested and it was found that by correctly choosing the thickness and density of the material the reflected wave could be virtually eliminated. Guy (1973) investigated shock-wave attenuation in a sudden enlargement in a duct with an absorbent lining. Pressure measurements on the axis of the tube showed elimination of the high frequencies, resulting from the removal of the multiple transverse waves.

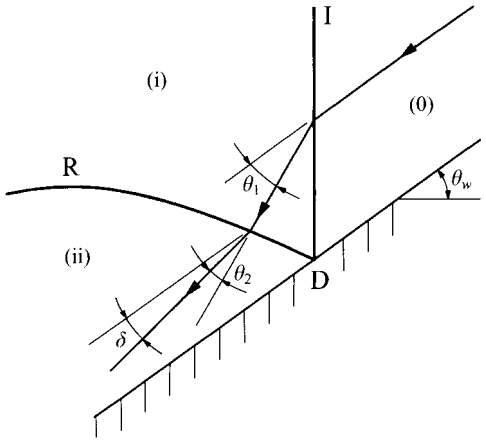

FIGURE 1. Regular reflection over a surface with inflow, in a frame of reference fixed in the point of reflection.

Clarke (1984) undertook a number of theoretical studies of oblique reflection off a porous surface, restricted to very weak waves. He assumed that the flow in the porous material followed Darcy's law with the interaction resulting in a reflected expansion wave terminated by a shock wave. This model is based on the premise that the material acts by swallowing or regurgitating air until such time as the pressures within the material are uniform and equal to the external air pressure. The expansion wave implies an inflow velocity greater than the component of velocity normal to the surface that is induced behind the incident wave. It was shown that flow in the material can be adequately described by using a momentum equation that combines Darcy's law with an inertia term. Bray (1984) conducted experiments with weak waves ($M = 1.08$) using slabs of polyurethane foam to compare with Clarke's predictions. It was found that the presence of the porous material inhibits the formation and growth of a reflected shock, and gives rise instead to a reflected continuous compression wave. He also showed that the effects of surface openness and foam depth are significant.

The current work is an extension of that of Onodera & Takayama (1990*a*, *b*). They examined the reflection of a plane shock wave from the surface of a slit wedge. Their main interest was in the transition conditions from Mach reflection to regular reflection over a wide range of incident Mach number conditions. This was done by running successive tests with increasing wedge angles from zero until regular reflection was obtained. For the stronger shocks ($M = 3$) and a surface perforation ratio of 0.4 it was shown that the transition angle was decreased by about 10° from that for a smooth rigid wall. These authors recognized that the flow behind the reflected shock may be unsteady because of wall suction, but for purposes of analysis assumed that in the vicinity of the reflection point the flow could be treated as quasi-steady. It is interesting, however, that they found the Mach stem to grow linearly with time in spite of its possible attenuation due to the expansion waves from the slits and thus the experiments may be assumed to be conducted at a high enough value of L/x to be treated as being quasi-steady. The steady-flow analogue in the corresponding shock-fixed coordinates is then as indicated in figure 1. The shock polar analysis corresponding to this flow was then used by these authors with the further assumption that, in plate-fixed coordinates, the flow into the plate is normal to the surface. The validity of this assumption will be dealt with later. An empirical matching coefficient was found to be necessary to get agreement between experiment and the shock polar analysis.

An experimental study of the general gasdynamic behaviour following shock-wave impact on a porous wedge has recently been reported (Skews 1994). Specimens of rigid porous material (silicon carbide and alumina) and a range of wedge angles were tested over a range of Mach numbers from 1.1 to 1.7. The external flow field was determined through schlieren photography and the conditions within the material inferred from wall pressure measurements. Substantial changes in reflected wave angles compared with smooth walls were noted, particularly in the case of regular reflection. For example with an inverse shock pressure ratio (upstream pressure/downstream pressure), $\xi = 0.7$, and a wedge angle of 40° the reflection angle decreases by about 25°. Some tests at $M = 1.51$ showed the triple-point trajectory to be a straight line within the accuracy of measurement. The general appearance of the external flow was very similar to that for a rough, but impervious, wall.

Kobayashi, Adachi & Suzuki (1995) conducted a theoretical and experimental investigation of shock-wave impact on porous surfaces with the emphasis on regular reflection conditions. Two different porous layers were tested, one consisting of spherical glass particles with a bed porosity of 44%, and the other a foam rubber with a porosity of 98%. Data were presented of the reflected shock angle for varying incidence angles and Mach numbers of 1.2 and 1.41. Two types of analysis were done, in both cases assuming that the flows are pseudo-stationary. In the first, flows within the porous material were ignored and calculations done for arbitrary values of δ (the 'sink effect' shown in figure 1) to see whether this could account for the observed wave angles. It was found that there were experimental results which could not be accounted for in this manner as the values of δ would be unacceptably large. The second approach was to examine the two limiting cases for inflow, such as done by Skews (1991) for the one-dimensional case. These limits are for $\delta = 0$ corresponding to a porosity of zero (conventional regular reflection from an impervious wall), and an infinitely weak (sonic) reflected wave corresponding to unity porosity. It was found that the experimental results for the 0.98 porosity material corresponded well with this latter case.

From a theoretical point of view, the recent work of Li, Levy & Ben-Dor (1995) is of significance. They analysed the regular reflection of a shock wave from a porous surface, also on the assumption that the process is pseudostationary as did Clarke, which therefore could be treated as a stationary reflection pattern in a steady supersonic flow. They assumed that in the vicinity of the point of reflection, where measurements are made, there is no momentum and energy interchange between the solid phase and the gas, and that these effects only become significant when the gas has propagated well into the pores, and there are thus minimal forces acting on the surface layer. A transformation is employed which treats the gas in the pores only, following which the usual shock relations are applied. The comparison of their results with the unsteady experimental data of Skews (1994) and Kobayashi *et al.* (1995) showed very good agreement, thereby indicating that the similarity assumption is a good approximation. The analysis in the present paper is also done using this assumption.

The view presented by Li *et al.* that the reflection process in the vicinity of the reflection point is not influenced by the frictional effects within the body of the material contrasts with the assumption (van Dongen *et al.* 1993) that when a shock wave hits a high-porosity foam there is almost no instantaneous reflection, and that the reflected wave is generated from within the body of the material because the gas that enters the foam decelerates due to friction. Which of these effects is dominant will probably depend on the nature of the surface as well as the porosity.

From the above it is clear that there are a number of effects which influence the

reflection process of a shock wave from a permeable surface. These are geometrical surface roughness and pore size effects, mass inflows into or through the material due to porosity, and bulk flow effects in the body of the material which feed influences back to the surface. This paper studies flows in the vicinity of the surface in detail, with an idealized geometry consisting of a plate with transverse slits.

2. Experiments

Tests were conducted with shock waves having nominal inverse pressure ratios of $\xi = 0.4$, 0.5 and 0.7, corresponding to Mach numbers of 1.51, 1.36, and 1.17 respectively, and over the full range of wedge angles from 0 to 90°. Owing to the experimental set-up and scatter, average Mach numbers and standard deviations were 1.540 (0.006), 1.382 (0.009), and 1.185 (0.009).

The main experimental facility used was the diaphragmless shock tube at the Shock Wave Research Center of the Institute of Fluid Science, Tohoku University. This unit has a low-pressure section with a cross-section of 60×150 mm. The high-pressure section is a concentric chamber situated around the driven section and connected to it via a flexible rubber diaphragm which acts as a valve at the inlet to the driven tube. This valve is controlled by the pressure in a separate chamber whose pressure is released by a bursting disk (Yang, Onodera & Takayama 1994). This tube gives a very good reproducibility in Mach number of about 0.2% and has the added advantage of not leaving diaphragm fragments in the tube. Experimental scatter in the current tests is slightly larger than this figure due to the incorporation of some earlier Mach reflection tests done in 1986 by Onodera using a conventional shock tube. Nitrogen was used as the test gas.

The models used are essentially those used previously by Onodera & Takayama (1990*a*, *b*) for their study on slit wedges. They consist of a circular arc holder to which different 2.25 mm thick plates can be attached. The plates are accurately machined using wire cutting, with a series of slits as indicated in figure 2. The holder is attached to the two acrylic windows of the shock tube and the whole window/model assembly is rotated in order to change wedge angle. Two test plates were manufactured and tested. The first, which will be referred to in this paper as the coarse (C) model, had 35 slits, each 1 mm wide, separated by 1.5 mm wide solid bars, giving an open area ratio of 40% over the slit surface, and the second had 58 0.5 mm slits separated by 1 mm bars. This model thus has a 33% open surface area and is referred to as the fine (F) model. Photographs of the models are given in Onodera & Takayama (1990*b*). A narrow rim runs down the edges of the plates connecting the bars in order to retain structural integrity. As noted by these authors this rim gives rise to a reflected wave in a different plane to that of the porous surface and care must be taken in measuring up the photographs. The effect of this wave distortion was found to reduce accuracy of measurement in the present work and future studies should avoid this effect by, for example, countersinking the ribs into the acrylic window material. The original models used by Onodera & Takayama were 2.25 mm thick but were plastically deformed under conditions of high shock loading. A second set of models were made with the same plate thickness but with a narrow stiffening web along the lower outside edges. It is for this reason that in the photographs published in their papers, the models appear proportionately much thicker than those in this paper. It should be noted that there are errors in the information given on the model sizes in the above references, the thickness t referring to the web rather than the plate thickness, and the slit width being 1.0 rather than 1.5 mm for the second model. For the present tests these stiffening ribs

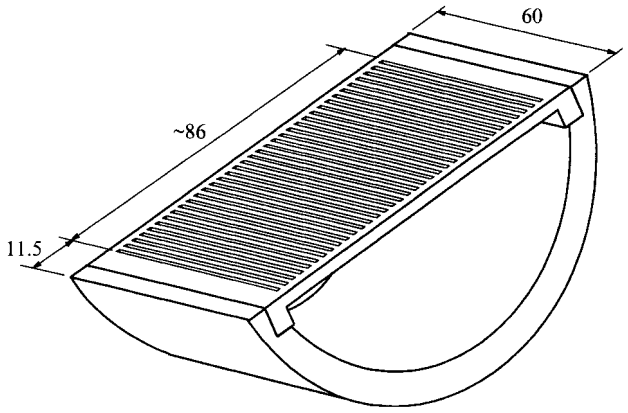

FIGURE 2. Design of the test model (dimensions in mm).

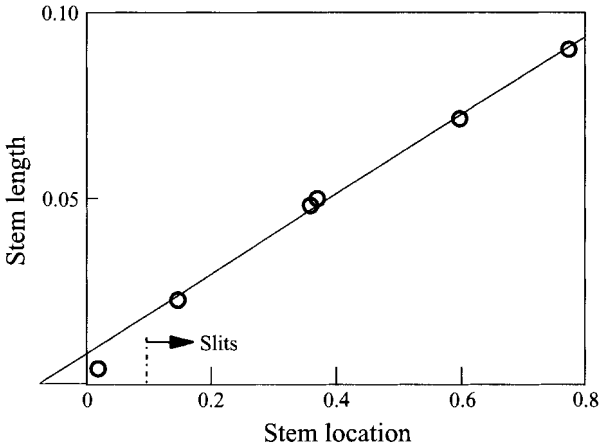

FIGURE 3. The triple-point trajectory. Stem length and location are non-dimensionalized with respect to the wedge length (Onodera & Takayama 1990*b*). $M = 1.53$, $\theta_w = 25.5°$.

were removed in order to make the full transmitted flow visible immediately below the surface of the plate, with the severe loading conditions being alleviated by running the tube at lower initial pressures: 1 bar for $\xi = 0.7$, 0.5 bar for $\xi = 0.5$, and 0.3 bar for $\xi = 0.4$.

Owing to the method of mounting of the plates there is a short length (11.5 mm) of unperforated material between the leading edge of the wedge and the start of the slits (figure 2). The effects of this were studied by Onodera & Takayama (1990*b*) and were established to be small under conditions of Mach reflection. Figure 3 shows their results for their measurement of the Mach stem length for a Mach 1.51 shock wave and a wedge angle of 26°. The stem length and shock location are non-dimensionalized with respect to the wedge length. It is seen that after an initial formation distance the triple point trajectory becomes straight. It was thus concluded that the wave system can be treated as being self-similar in time with an effective wedge apex upstream of the actual apex. This result is utilized in §4 to establish the velocity of propagation of the wall shock along the wedge surface for Mach reflection situations. This leading-edge influence is, of course, not a problem in regular reflection situations where the flow in region ii (figure 1) is supersonic with respect to the reflection point, as the reflection point then has no knowledge of the existence of the wedge apex.

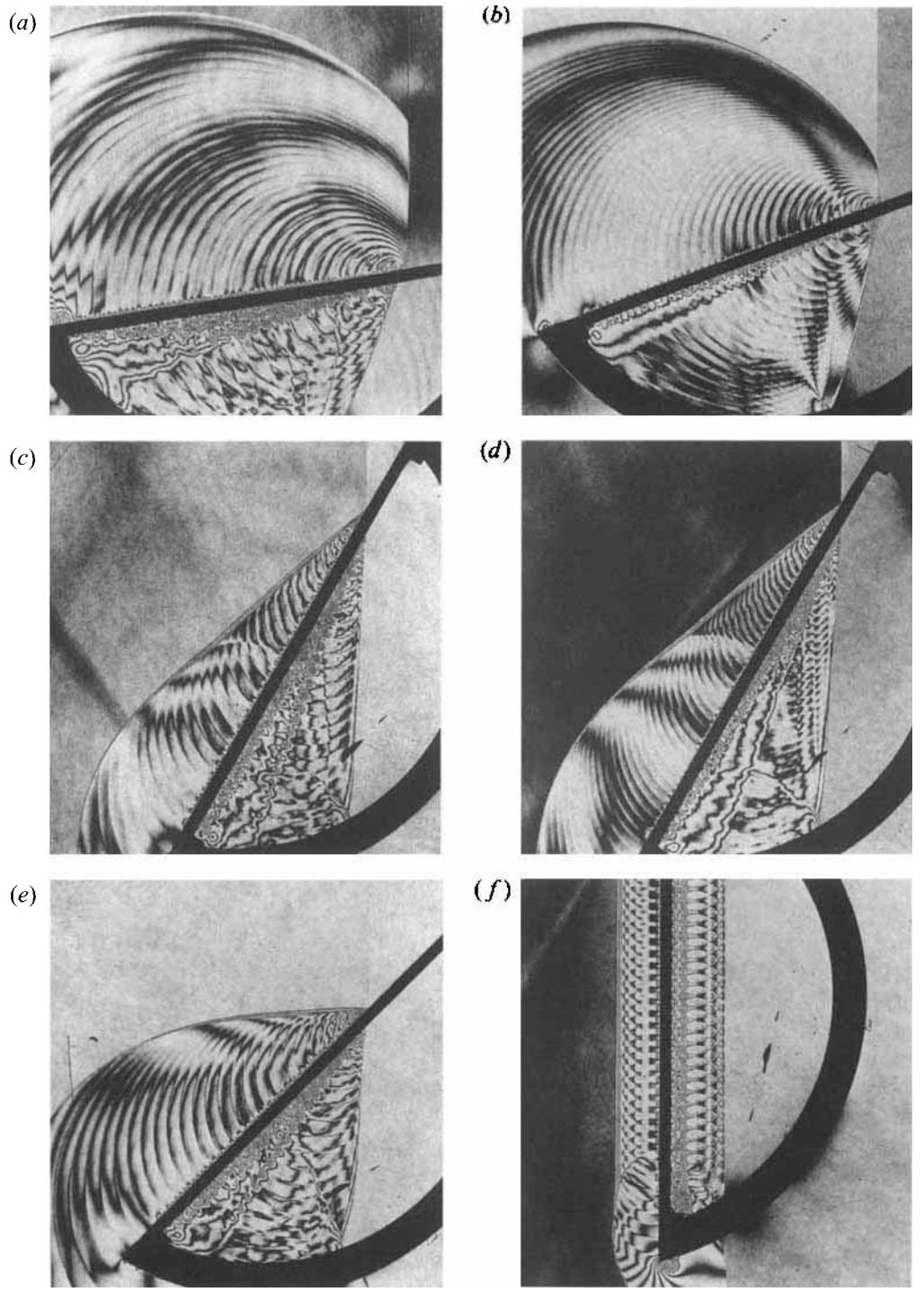

FIGURE 4. Typical interferograms. (*a*) $M = 1.37$, $\theta_w = 9°$, C; (*b*) $M = 1.18$, $\theta_w = 20.2°$, F; (*c*) $M = 1.54$, $\theta_w = 60°$, C; (*d*) $M = 1.54$, $\theta_w = 60°$, F; (*e*) $M = 1.39$, $\theta_w = 45°$, C; (*f*) $M = 1.38$, $\theta_w = 90°$, C.

The earlier tests of Onodera & Takayama covered wedge angles from zero up to about 45°, and thus dealt primarily with Mach reflection conditions, as their interest was largely in the effects of slits on the reflection transition process. Some of these previous results are included in the present analysis. Whilst some tests were repeated in this lower range the new tests were mainly in the regular reflection region, all the way up to the case of normal reflection corresponding to a nominally one-dimensional flow situation.

Double-exposure holographic interferometry, as implemented by Takayama (1983), was employed to record the wave interaction patterns. Although the fringes are isopycnics, they were not used in the present work to establish quantitative values of density, partly because of the very complex flows which makes it difficult, if not impossible, to count fringes. However, they were beneficial in improving the definition of the wavelets in the flow arising from the slits and in distinguishing between regions of low and high density gradients. Typical reconstructed images are shown in figure 4 for Mach reflection (*a*, *b*), regular reflection (*c*, *d*, *e*), and normal reflection (*f*).

3. Characteristics of the flow

The basic features of the flow are identified in figure 5, although as will be noted from the interferograms there are differences in the flows, depending both on Mach number and on wedge angle. Thus in this figure, which is a tracing of figure 4(*e*), there are three shock waves: the incident wave (I), the reflected wave (R) and the transmitted wave (T). In the case of Mach reflection there is the additional Mach stem shock (figure 4*a*, *b*). There are five major flow regions. First the unperturbed region (0) ahead of the shock, both above and below the plate, and secondly the uniform and undisturbed region (i) behind the incident shock. Then there is the disturbed region (ii) between the plate and the reflected wave, which is directly influenced by the flow through the plate and is traversed by the weak waves arising from the slits. There are two regions (iii) and (iv) below the plate separated by a contact surface. Region (iii) contains gas which has passed through the slits, and region (iv) is the gas engulfed by the transmitted shock wave as it is driven ahead by the contact surface.

3.1. *The flow above the plate*

The flow between the reflected wave and the surface of the plate is characterized by reflected wavelets arising from the interaction of the point of reflection with the surface. Examination of an interference fringe passing through these wavelets (e.g. figure 4*e*), show a zigzag pattern corresponding to a series of sharp-fronted compression fronts (shocklets) followed by expansion waves. The source of this pattern is easily understood from an examination of literature on the interaction of a shock wave with a branched duct or a bend in a duct (e.g. Skews 1971), which is a similar situation to the shock entering a slit in the present case, as well as Adachi *et al.*'s (1992) photographs on guttered wedges. A schematic of the expected flow in the vicinity of a slit is shown in figure 6, which is constructed from the above studies coupled with the numerical simulations done by Onodera & Takayama (1994), a similar schematic of Friend (1958), and the results of the current study. The shocklet results from the reflection of the incident shock wave from the far side of the slit and the expansion wave from the diffraction of the incident shock at the leading edge of the slit (one example is shown dotted), as well as the expansion of the shocklet flow in space (i.e. as a blast wave). Other waves resulting from flows on the lower side of the plate may enter this upper flow field through the slits and vice versa. Most of these re-reflected

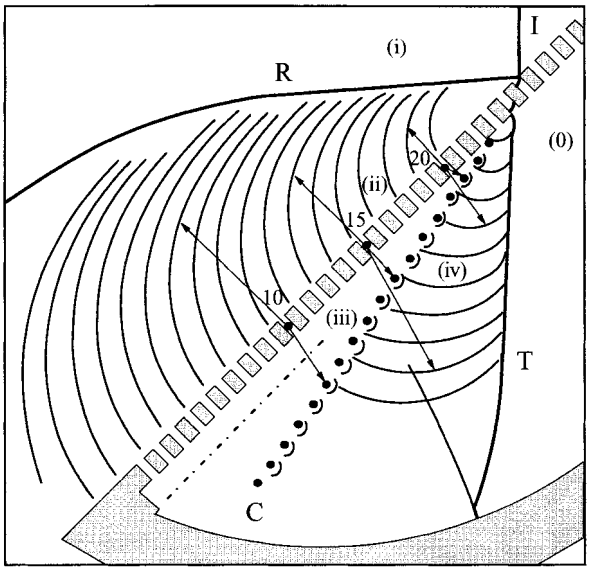

FIGURE 5. Characteristics of the flow. The arrows identify the wavelets and vortices arising from the 10th, 15th and 20th slit.

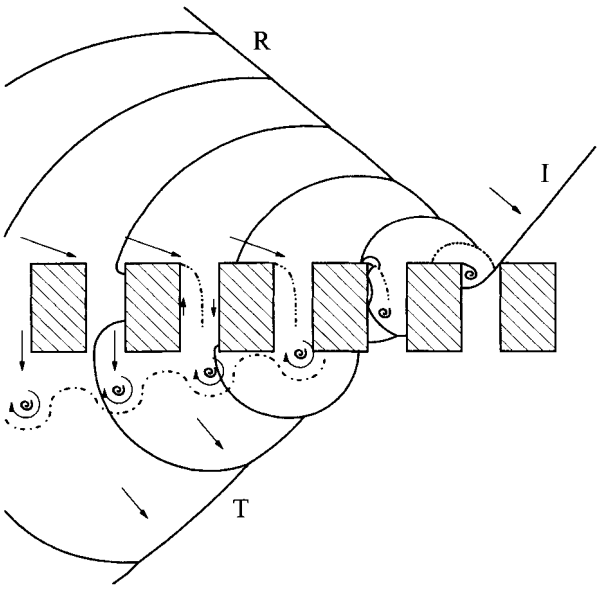

FIGURE 6. Schematic of the flow through the slits, with arrows showing the flow direction in a frame of reference fixed in the plate.

waves are not shown in the diagram as the flow clearly becomes very complex. The flow in the vicinity of the slits will be discussed in more detail in §5.

Careful analysis of the interferogram enables the slit which is responsible for each of the shocklets to be identified. In figure 5 this is done for the 10th, 15th and 20th slit, with the incident wave just having reached the far edge of the 25th slit. Inferences regarding the gas inflow motion will be made later using this information. It is evident, however, that the oscillations in density due to these wavelets is small (of the order of

one fringe shift), and the approximation may be made that the background density along each fringe is relatively uniform. The positions of the slits can be identified on the interferograms by the small semi-circular fringe patches on the upper surface of the plate. There are two of these from each slit, corresponding to the two corners of the slit, and they are visible because of the high flow gradients around these corners.

It is noted in the cases of Mach reflection that the Mach stem is not perpendicular to the wall. Whilst the tip of the wave is changing all the time due to successively striking a rigid wall and then a slit opening, the localized effect soon smooths out as the effects propagate up the stem. For low wall angles the Mach stem tends to lag the incident wave, whereas for higher angles, and stronger shocks, it leads, but in all cases the angle between the stem at the wall, and the wall, is less than 90°. The consequence of this is that the flow behind the stem must have a flow component into the wall. Furthermore it is interesting to note that no slipstream is discernable, presumably because it is dispersed owing to the Mach stem being made up of a myriad of reflections from each of the solid elements between the slits. Unfortunately the presence of the unperforated edges of the model result in multiple images of both the reflected shock and the Mach stem which influences the accuracy of measurement. It has been assumed that the leading wave in such multiple images is that from the solid rib.

For the larger wall angles in regular reflection (figure 4*c*, *d*, *f*) the point of reflection outstrips the corner signals, the front of which is clearly visible in the interferograms, and in these cases the only characteristic length associated with the phenomena is that of the slit width. The catch-up angle has not been specifically established but occurs with a wall angle in the region of 50°. The section of the reflected shock wave which cannot be influenced by the corner is straight, and these circumstances are the closest to representing a truly pseudosteady flow, and thus being appropriate for shock polar analysis. However, for the regular reflection shown in figure 4(*e*) the reflected wave is curved along its whole length.

One of the questions that does arise is the influence that the flow underneath the plate can have on the flow on the upper surface. It is clear that if the pores are choked then perturbations from under the plate will not be able to influence the upstream flows; however, if they are not, then the wave transmitted down through the slit will transmit a wavelet back to the upper surface as it expands on reaching the under surface. This effect has been noted by Suzuki & Adachi (1987), Onodera & Takayama (1990*a*, *b*), and Adachi *et al.* (1992) for cases where the bottom of the slits is closed. In such cases a shock wave is reflected from the bottom of the slit and emerges into the upper flow. What is of importance, however, is that for regular reflection from high wall angles this secondary disturbance does not influence the behaviour at the point of reflection itself, owing to the finite transit time of the disturbance into, and back up, the slit, and the high-velocity flow behind the reflection point, although it does influence the flow a short distance behind the reflection point. For Mach reflection the flow behind the foot of the Mach stem is subsonic and these secondary lower-surface wavelets can influence the stem shape. Some evidence of this reflected expansion wave from the bottom of the slit re-emerging into the upper flow is visible just behind the Mach stem in figure 4(*a*). For materials with randomly distributed pores this effect will become smeared throughout the flow, and a range of compressions and expansion waves with different arrival times will re-emerge to influence the flow.

3.2. *The flow below the plate*

The flow underneath the plate, between the transmitted wave and the lower surface of the plate is divided into two distinct regions (denoted as (iii) and (iv) in figure 5) by a

contact surface (C) made up of a series of vortices, the gas in region (iii) being that which has passed through the perforated surface. Examination of the interferogram shows that there is only one vortex per slit and not two as might be expected from consideration of the development of starting vortex rings during the impulsive starting of a flow through an orifice or nozzle. In the present case, as the incident shock diffracts into the slit the flow separates and rolls up into a vortex whose path should be very similar to that found in shock diffraction experiments (Skews 1967*b*) with the flow angle being dependent on the shock Mach number and wall turning angle. However, as the reflected shock from the far edge of the slit passes back over the vortex this will slow it down and the subsequent motion will be more in the direction of the slit (see figure 6). The existence of one emerging vortex rather than two is one of the indicators that the flow at the inlet to the plate is not normal to the surface, in a frame of reference fixed in the surface, as has been assumed in some previous work.

With a sufficiently thin plate, and with the inlet flow having a velocity component in the direction of the incident shock motion it could be expected that at the exit the flow would retain a forward component with respect to the plate. This is a central assumption in Friend's (1958) analysis where conservation of the tangential velocity across the plate is assumed, and is also an assumption contained in Li *et al.*'s (1995) analysis regarding conservation of tangential momentum. Since the vortex emerging from the plates gives an indication of particle motion, its trajectory will give an indication of the flow in its vicinity. It is noted that the vortex emerging from slit 20 in figure 5 emerges slightly forward of the centreline of the slit, indicating a slight forward velocity with respect to the plate. However, there is a slight backward drift of the vortex centre relative to the slit from which it emerged, as it moves away from the plate. The vortex from slit 15 is almost directly opposite its source slit, and that from slit 10 has been dragged even further back. This backward movement is a bit surprising in view of the fact that the shear acting on the line of vortices from the flow in the adjacent region (4) flow is strongly in the opposite direction. However, in view of the relatively small magnitude of this drift it would appear to be acceptable in theoretical modelling to assume the flow to leave the lower surface normal to the face. Whether this would only apply to plates with slits and geometries which impose strong flow guidance, as in the present case, or is more generally true, has still to be established. A similar schematic given by Friend (1958) shows a forward drift, but in view of inaccuracies in that diagram this may not be intentional. In the present case there thus appears to be a fairly rapid turning of the flow within the slit, a turning which would probably be more gradual, if it occurs at all, in a more isotropic and homogeneous material.

As the vortices move away from the plate they become less well defined and eventually vanish, although the interface between regions (iii) and (iv) remains easily distinguishable. The only differences between test conditions for figures 4(*c*) and 4(*d*) is the slit width. Note that the smoothing out of the discrete vortices occurs, for both cases, at the position of approximately the twentieth vortex from the shock position. The flow in the vicinity of the contact surface is clearly complex, because in addition to the shear the surface is convoluted owing to the presence of the vortices. Such a flow system cannot persist and must breakdown through mixing. In addition it is seen in the interferograms that there is a region of highly disturbed flow adjacent to the lower surface which is approximately of fixed width parallel to the plate, and thus appears to be the formation of the steady wake of the flow passing through the slits. The coalescence of a number of jets from multiple holes in close proximity has been noted before and is commented on by Ward-Smith (1971). In any event it can be expected

that as long as the pressure difference is maintained across the plate a steady flow situation with a fixed-geometry jet efflux will develop. It is expected that this would show as features parallel to the plate.

Complex interactions of the shock wave occur within each of the slits as indicated in the second slit of figure 6, but on exit diffract into approximately cylindrical surfaces. Those moving into the ambient air soon merge to become the plane transmitted wave (T). This wave may also be regarded as being the result of the contact surface acting as a gas piston and pushing the wave ahead of it. Wavelets similar to those above the plate are evident in this region. The fringes also tend to show a zigzag-type pattern resulting from the expansion of these hemispherical fronts. The wavelets are weak and will move at a speed close to sonic velocity whilst at the same time being convected with the background flow in region (iv). The centres of these approximately circular wavelets tend to lie on the line of vortices, as is to be expected, but do not lie on the vortex arising from the same slit as the wavelet originated from because of the shear along the contact surface.

The flow on the underside of the plate is slightly confounded by the reflection of these wavelets from the inner curved surface of the mounting frame. However, these wavelets are weak, as is evidenced by the minimal distortion they cause to the incoming wavelets, except where they conglomerate to form a reflected shock wave. This occurs sufficiently far from the measurements of the straight portions of the transmitted shock and contact surface so as not to influence the results. However, as will be noted later, the gradients caused by this series of small compressions can have the effect of curving the contact surface.

It is apparent, particularly for small plate angles, that the wave is slowed considerably whilst it is passing through the slits, as the point of emergence of the wave on the underside of the plate is somewhat behind the point of entry. No attempts are made in this work to quantify this effect because the plate is too thin to obtain reasonably accurate measurements.

4. Analysis

Analysis is conducted in two frames of reference, which need to be clearly distinguished from each other. The one is the laboratory frame, where the plate is stationary, and velocities relative to the plate are considered. Such velocities will be denoted with asterisks as V^*. The second frame is fixed in the point of shock disturbance (D) (see figure 7) moving along the upper surface of the plate, and thus for regular reflection is simply the point of reflection, whereas for Mach reflection it is the foot of the Mach stem. This is somewhat different from the usual transformation used for Mach reflection where the flow is defined with respect to the triple point. However, in the present case the triple-point motion has little relevance to the flows through the plate in the vicinity of point D. For both cases it is assumed that the wave patterns remain similar in time, and thus this second frame of reference will be referred to as the 'steady' frame since the flows in the vicinity of the point of disturbance remain invariant in time, although this is not an exact description since in the Mach reflection case the triple point is receding from the foot of the Mach stem. The transformation from one frame to the other is obtained simply by superimposing a velocity V_D (the velocity of point D along the plate), in the direction of the surface of the plate.

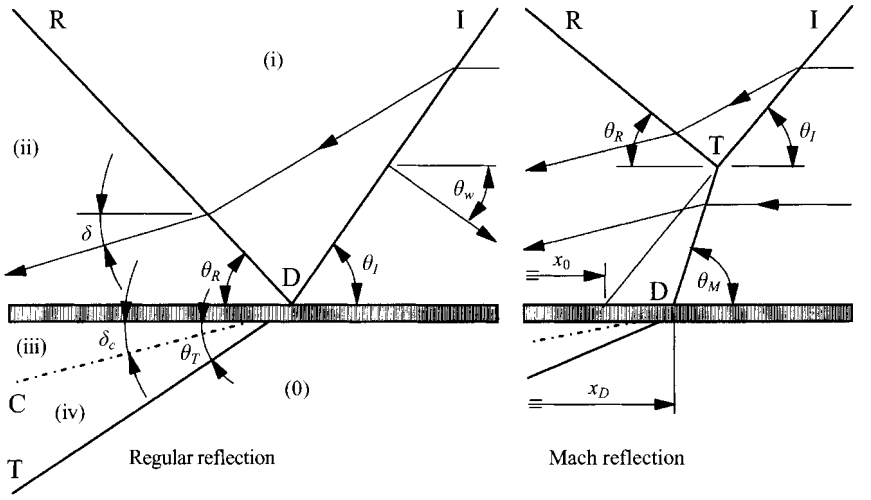

FIGURE 7. The flow geometry and definition of symbols for regular and Mach reflection.

4.1. *Analysis based on wave geometry*

It is assumed that all waves and the contact surface are straight and separate regions with uniform properties. Special treatment has to be given to the case of normal reflection since V_D becomes infinite. Simple one-dimensional analyses are applied in that case.

For regular reflection

$$M_D = \frac{V_D}{a_0} = \frac{M_I}{\sin\theta_I}, \tag{1}$$

where M_I is the incident shock Mach number (laboratory frame), a_0 is the sound speed in the gas ahead of the shock, and θ_I is the shock incidence angle, and is the angle complementary to the wall angle. A correction has to be applied to the above equation in the case of Mach reflection. An estimate is made of the effective length of the test wedge from data such as that of figure 3. The above equation is then multiplied by the ratio x_D/x_0 (figure 7), where x is measured from the effective apex. This correction is small and in all the tests conducted does not exceed 4% for lagging Mach stems and 3% for leading waves. Note also that measurements in the Mach reflection case are restricted to photographs with a significant length of Mach stem to enable the incidence angle on the plate to be measured with reasonable accuracy. M_D is thus also the Mach number of the oncoming flow, parallel to the surface of the plate, in the steady frame of reference.

The deflection of a streamline through an oblique shock wave is given by

$$\tan\delta = \frac{(M^2\sin^2\theta - 1)\cot\theta}{M^2[\frac{1}{2}(\gamma+1) - \sin^2\theta] + 1}, \tag{2}$$

where γ is the ratio of specific heats, and the Mach number on the downstream side by

$$M_{new} = \left(\frac{2+(\gamma-1)M^2\sin^2\theta}{2\gamma M^2\sin^2\theta - (\gamma-1)}\right)^{1/2} \operatorname{cosec}(\theta-\delta), \tag{3}$$

where M is the oncoming flow Mach number and θ is the angle of this flow to the shock wave. A single application of these equations across the Mach stem for Mach

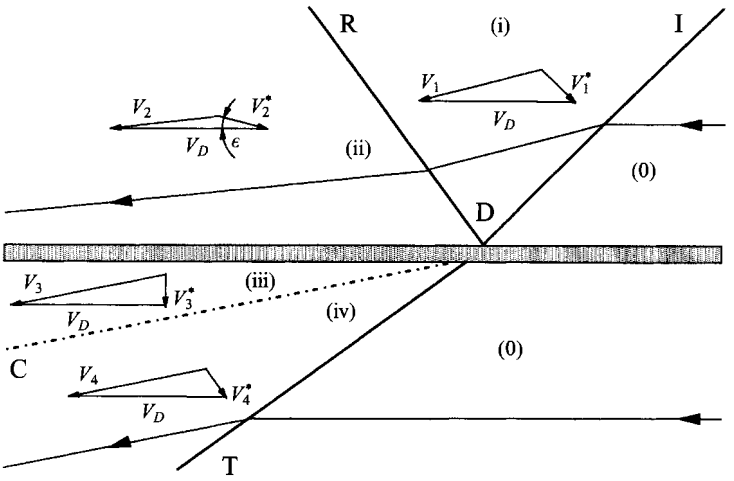

FIGURE 8. Velocity triangles connecting the frames of reference. Velocities with asterisks are in a frame fixed in the plate, and the corresponding velocities without asterisks are in a frame fixed in the point D.

reflection, and a double application for regular reflection, first across the incident shock and then across the reflected shock, using the measured shock angles at the wall, gives the steady flow magnitude and direction in region (ii) just above the plate. A corresponding single application across the transmitted wave gives the conditions in state (iv). Calculation of the sound speed ratios from

$$\frac{a_y}{a_x} = \left(\frac{1+\frac{1}{2}(\gamma+1)M_x^2}{1+\frac{1}{2}(\gamma+1)M_y^2}\right)^{1/2} \tag{4}$$

then enables the steady flow velocities in each of the regions (i), (ii), and (iv) to be determined.

The velocity triangles connecting the two frames of reference are shown in figure 8. Conditions in state (iii) are determined on the assumption that the flow at the exit from the plate is normal to the surface in the laboratory frame of reference (V_3^*) as inferred from the starting vortex motion, and parallel to the contact surface in the steady frame of reference (V_3). V_1^* and V_4^* are normal to the incident and transmitted shocks, being the induced velocity behind a plane wave moving into ambient air. The magnitude and direction (ϵ) of V_2^* are the main parameters to be determined from the experimental results as they quantify the inflow into the plate. The current analysis does not assume that the flow directions in regions (iii) and (ii) are the same, nor than the inflow into the plate is normal to the surface, as has been done previously.

4.2. *Analysis based on wavelet motion*

Further information about the inflow may be obtained from an examination of the behaviour of the wavelets. As discussed above, these shocklets are essentially acoustic fronts arising from the shock reflection off the far edge of each of the slits. After being generated they will distort and be convected with the flow depending on the surrounding temperature and velocity field. It is noted from the interferograms that in the vicinity of the wall the wavelets are not normal to the wall, thereby indicating a migration of the surrounding flow into the wall. The situation is illustrated in figure 9. Consider the shocklet generated when the main shock reflection point passes the edge of a slit at S. At the time depicted in the diagram the reflection point will have moved

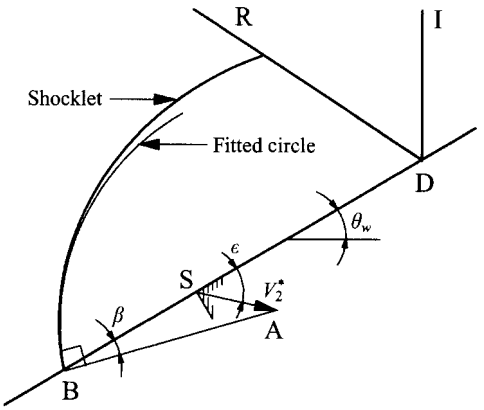

FIGURE 9. The effect of wall inflow on the shocklet motion. The centre of curvature of the weak shocklet is convected from S to A as the shock reflection point moves from S to D.

to D and the shocklet front will have moved outward to intersect the wall at B. Assuming that the flow in the vicinity of the wall remains at the values determined above, the centre of the wavelet will move from S to A at a velocity V_2^*, and along a path at an angle ϵ to the wall. The distance SA is then $V_2^* t$, where t is the time taken for the incident shock wave to move from S to D, and may be calculated knowing the shock Mach number and wall angle. The distances DS and BS are measured from the photographs with S being identified from the concentration of fringes due to the high density gradients at the inlet to a slit. From the above data the wavelet inflow angle β may be determined. This is then compared with the measured values. Measurements were made using a transparent template with a series of concentric circles inscribed on it, and the circle best fitting the curvature at B used to determine the direction of BA. Note that no assumption has had to be made about the distance BA, which represents the local sound speed, as it is simpler and more accurate to determine the perpendicular to the shocklet at B than the radius of curvature. The method is subject to some variability: $\pm 1°$ for the smaller wall angles where the wavelets are closer to being circular (see figure 4*a*), and up to $\pm 2°$ for larger angles (figure 4*c*) due to the shortness of the arc. Measurements were taken from three or four different wavelets arising from different slits between the 9th and 18th slit for each photograph, with the shock positioned typically at about the 30th slit, and the results averaged. These measurements were only done for the coarse model with $\xi = 0.4$. Similar calculations could be done for the wavelets behind the transmitted wave but are found not to be necessary because of the correlation between the contact surface angle and the flow angle determined from the transmitted shock slope as discussed below.

In the case of normal reflection simple one-dimensional calculations are employed. The photographs are taken so that an undisturbed portion of the incident shock wave is visible. Knowing the velocity of the incident wave enables the absolute velocities of all other features to be easily determined by simply taking ratios of distances measured from the photograph.

5. Results and discussion

The effect that surface properties has on shock reflection phenomena is usually quantified by the comparison of incident and reflected shock angles. Figures 10(*a*) and 10(*b*) show the results of the present tests for $\xi = 0.7$ and 0.4, compared with the

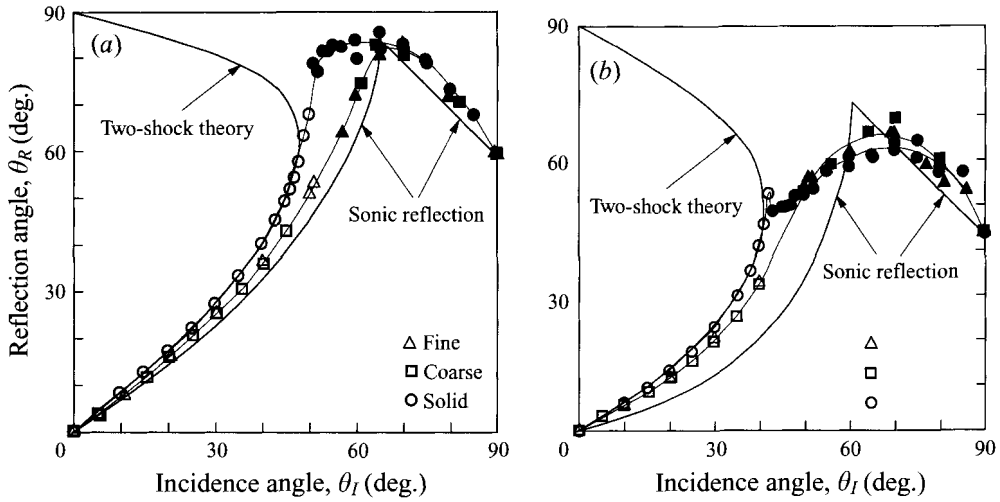

FIGURE 10. The reflection behaviour for (*a*) $\xi = 0.7$, and (*b*) $\xi = 0.4$. Solid symbols represent Mach reflection and open symbols regular reflection.

experimental results of Smith (1945) for a smooth wall (shown by circles), the two-shock theory of von Neumann (1943), (corresponding to a wall with zero porosity and inflow), and the theoretical solution for a sonic reflected wave (corresponding to unity porosity and complete inflow corresponding to that behind the incident shock). This latter limiting case is made up of two components, the first (lower incidence angles) corresponding to supersonic flow behind the incident shock relative to the reflection point and the reflected wave simply being a Mach line in this flow, and the second being for subsonic flow where the reflected acoustic wave consists of a semicircular front behind the shock, intersecting it at a position described by Skews (1967*a*). It should be noted that the presentation of the present results is different from that usually employed in that the shock angles in Mach reflection are measured with respect to the wall rather than with respect to the triple-point trajectory. This is because the current concern is with the inflow at the wall which is controlled by the angle of the foot of the Mach stem, and thus the triple-point trajectories were not determined, and because the issue of transition has already been dealt with by Onodora & Takayama (1990*a*).

As expected for regular reflection, the results lie between the impervious-wall case and the sonic reflection limit, and the result of the wall permeability is to lower the reflection angle. Because of the close proximity between the zero inflow and complete inflow limits shown by these figures, particularly for the weaker incident waves, it is evident that it will be experimentally difficult to accurately determine the effect of porosity based on wave angle measurements. It is largely because of this that the present results show no detectable difference between the coarse- and fine-slit test models (porosities of 0.4 and 0.33). Kobayashi *et al.* (1995) have shown that for an open-pore rubber with a porosity of 0.98, the results lie very close to the sonic reflected wave limit. Li *et al.* (1995) have successfully correlated these results and those of Skews (1994), which were for relatively thick specimens of the order of tens of pore diameters, with their theory. Unfortunately their theory depends on a knowledge of the tortuosity of the material, which is not a pertinent concept in the present context.

For the impervious-wall tests there is quite a marked change in the slope of the reflection curve at transition to Mach reflection. This change is not apparent for the perforated surface. Because of the complex unsteady flow field close to the wall, with

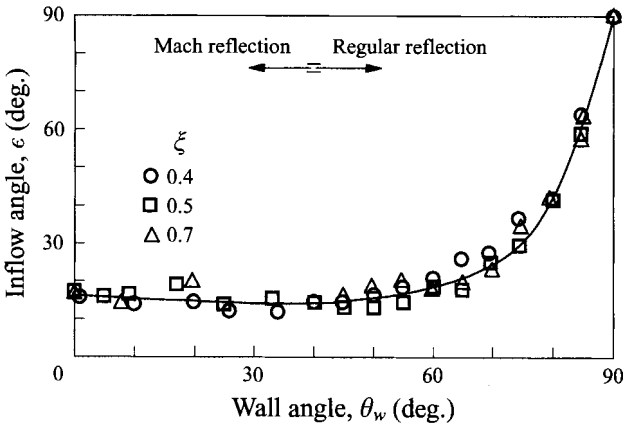

FIGURE 11. The variation of the inflow angle for the coarse model.

a length scale corresponding to the slit size, it is not possible to define transition as distinctly as for a smooth wall and it could therefore be expected that the change from the one type of reflection to the other would be more gradual. It is interesting to note from figure 10 that for a large portion of the Mach reflection regime, particularly as glancing incidence is approached, there is no significant difference between solid and perforated walls. It is clear that all the results, no matter what the wall condition, must converge to the theoretical value for an incidence angle of 90°, since the reflected wave must then be an acoustic wave, and its geometry will be as given in Skews (1967*a*).

The direction of inflow into the wall is shown in figure 11. Notwithstanding the sparsity of data in the region of transition owing to the difficulty in measuring the angle of the Mach stem when it is short, it is interesting to note that the value of ϵ (figure 8) is continuous across transition, remembering that the method of calculation is different for the two cases: for Mach reflection the deflection is determined across a single shock, whereas for regular reflection the calculation is across two shocks. The most striking result evident in this figure is that over a large range of wall angles the flow direction into the wall is shallow and constant (about 17° for wall angles from zero to nearly 60°). This is in marked contrast to the assumption in some previous theoretical work that the inflow is normal to the wall. Thus these theoretical models need to be treated with considerable caution. The experimental curve is independent of Mach number for the Mach numbers tested and is also not affected by the differences in porosity of the test models used. The results are not shown for the fine model since the results could be expected to be the same as the coarse model as the wave geometries are the same (figure 10). It is pertinent to note that for plane-shock diffraction around a convex corner (Skews 1967*b*) which corresponds to the present case for $\theta_w = 0°$ and a turning angle of 90°, the slipstream (separation) angle, which corresponds to the angle of the flow into the slit, is of similar magnitude to the inflow angle found above. Also for diffraction of a shock with $\xi = 0.4$ over corners from 45° to over 90° the flow separates along a streamline at an angle of between 12° and 20°. Whilst the situation is not quite the same since the incident shock is inclined to the surface of the plate in the present case, it appears that the induced flow behind the successive diffractions at each slit could be due to the slipstream angle resulting from the diffraction. More detailed experiments at larger scale would be needed to establish separation angles for diffraction into a branched duct when the incident wave is inclined. The flow conditions that may prevail at a surface with non-uniform and randomly distributed pores

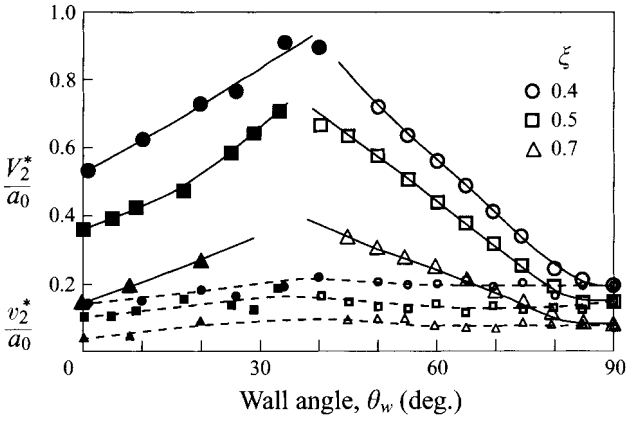

FIGURE 12. The magnitude of the inclined inflow velocity, and its component normal to the plate. Solid symbols represent Mach reflection and open symbols regular reflection.

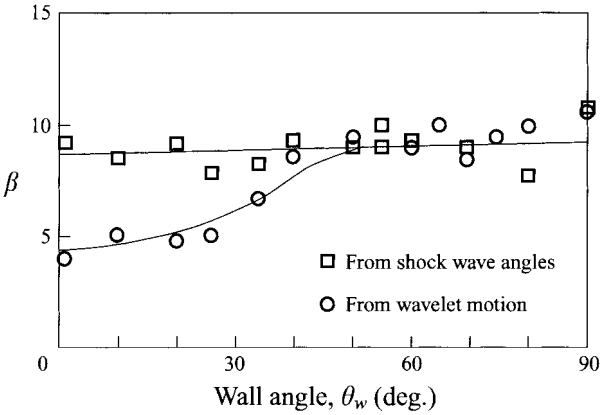

FIGURE 13. The wavelet angle as determined by the two independent methods of calculation.

requires further study, but it is evident that assumptions regarding the inflow direction should not be made, either in theoretical nor experimental studies.

The magnitude of the inflow velocity, V_2^*, is shown in figure 12. The major point of note is that maximum velocities are reached in the vicinity of transition, with a fairly marked drop on either side, and with higher velocities being associated with higher incident Mach numbers. The component of this velocity normal to the plate, v_2^*, is also shown. This is much less variable than V_2^*, particularly in the case of regular reflection beyond the catch-up angle ($\approx 50°$) where it is almost constant, and thus the change in the inflow velocity is brought about primarily through the change in the component parallel to the plate, u_2^*. For lower wall angles, changes in the values of v_2^* are matched by proportional changes in u_2^*, leading to the constancy in ϵ.

The results from the independent wavelet-motion method of inferring inflow conditions, and which does not depend on shock geometry, are given in figure 13. From a wall angle of about 45° upwards the results agree very well with the results determined from shock-wave angle measurements, but for low wall angles there is a significant difference of about 4°. The essential difference between the two methods is that one is calculated from the shock reflection conditions and thus should be valid immediately behind the shock reflection point, whereas the other is from wavelet geometry well behind the reflection point. The agreement for the larger wall angles is

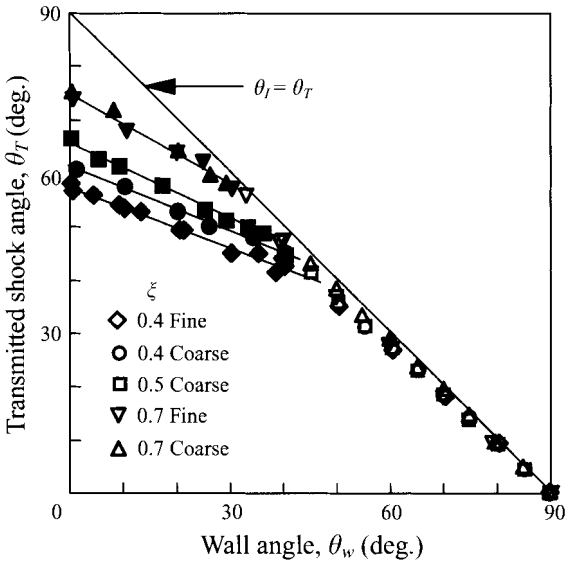

FIGURE 14. Variation of the angle of the transmitted shock wave. Solid symbols represent Mach reflection and open symbols regular reflection.

not unexpected, particularly for wall angles beyond the catch-up angle. The reflected shock is plane and the flow between it and the wall will be uniform except for the small perturbations due to the wavelets, and thus any method of measurement of inflow within this region should give similar results. Unfortunately the fringes in the flow do not help with this interpretation since what appear to be multiple fringes are simply the same fringe between successive wavelets. On the other hand, for the Mach reflection situation there are a number of factors which could contribute to a change of inflow conditions well behind the shock compared to those immediately behind the foot of the Mach stem. For short Mach stems there is a discontinuity in shock slope at the triple point, and even though a slipstream is not apparent there must be a gradient of properties which propagate down to the wall. For longer stems such as those shown in figures 4(*a*) and 4(*b*) the stem is curved and thus the properties behind are variable as can be seen from the fringes in figure 4(*a*). It must thus be concluded that the inflow will change in Mach reflection down the length of the wall and the data for β presented in figure 13 are an average value dependent on the positions where the measurements were made. During the measurements for a specific test there was an indication that the value of β decreased as the measurement point moved away from the foot of the Mach stem in accordance with the above conclusion, but the accuracy of measurement and variability in wavelet shape do not allow this to be stated with any confidence, and the averaging described in §4 hides the variability.

The above discussion concerns results which may be obtained from consideration of the flow above the plate alone. A similar approach will be applied to the flow under the plate, and then the flow conditions across the plate will be dealt with. Thus the flows in regions (iii) and (iv) may be obtained, on the assumptions that the flows in these regions also are uniform, that in the steady frame of reference the flows in both regions are parallel to the slipstream, and that the slipstream cannot sustain a pressure difference.

The angle of the transmitted shock is given as a function of the incident shock angle in figure 14. If there were no attenuation across the plate, the reflected wave would be

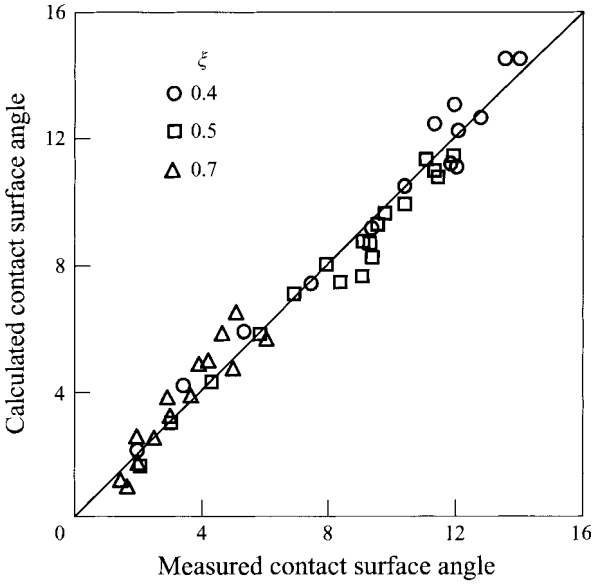

FIGURE 15. The contact surface and vortex street angle as measured from interferograms, and as calculated from the transmitted shock wave angles.

a sound wave and the transmitted wave angle would be the same as the incident angle for the case of regular reflection. The small deviation for this case is thus an indication of the small loss across the plate. (The same conclusion cannot be reached for Mach reflection since the strength of the foot of the Mach stem does not correspond to that of the incident shock.) Thus even for plates with substantial blockage such as in these tests (60% for the coarse model, even without taking the vena contracta into account) there is still substantial inflow, and the processes near the reflection point at the surface may not be influenced much by viscous effects. The diffraction process into the slits also involves little loss as is confirmed by the success of the inviscid Euler equation solutions for such a process. These factors may be part of the reason for the success of the theoretical model of Li *et al.* (1995) in predicting reflection from porous materials.

It is also noted that the transmitted wave resulting from Mach reflection on the upper surface is relatively less strong than for regular reflection, as evidenced by the lower slope of the experimental curve, because of the reduced mass flow through the plate resulting largely from the more glancing impact of the shock. The Mach stem does not bend strongly forward to be normal to the surface as it does for an impermeable plate; in fact in many cases its strength is close to that of the incident wave due to the interaction with the expansion waves arising from the slits. As will be shown, the pressure driving the gas through the plate is less and the transmitted wave consequently weaker. It is this reason that also accounts for the reduction in inflow velocity noted above. There is some evidence of a difference between the coarse and fine plates as would be expected, but this is only significant at the highest Mach number tested. Thus a much wider range of blockage areas would need to be tested in order to find the effect of porosity.

Treating the transmitted wave as an oblique plane wave in a steady flow enables the conditions in state (iii), figure 5, to be determined. For the Mach reflection case it is assumed that the disturbance moves up the plate at the Mach number M_D as described previously. In the steady frame of reference the flow in region (iii) should be parallel to the contact surface. Figure 15 shows the correlation between the measured contact

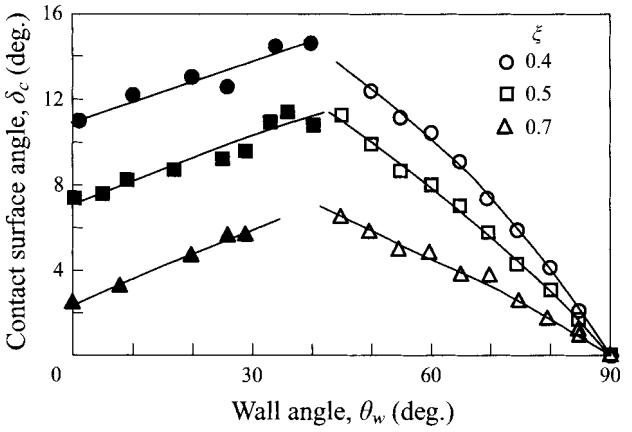

FIGURE 16. The contact surface angle on the underside of the plate.

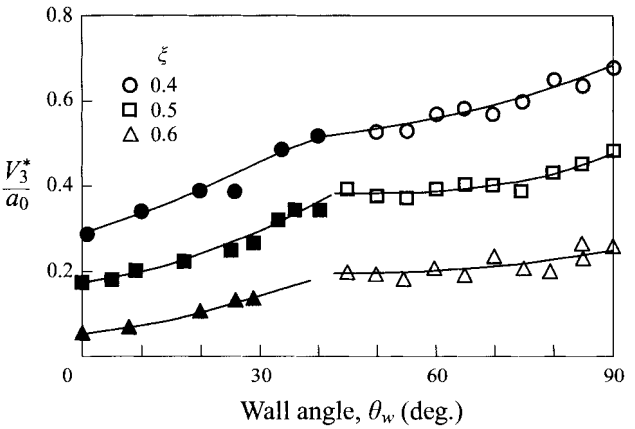

FIGURE 17. Outflow velocity normal to the plate.

surface angle δ_c (figure 7) and that calculated from the transmitted wave angle. The correlation is good considering the accuracy with which the angle can be estimated in the interferograms, and thus the assumption that region (iii) is uniform appears to be valid. For the low Mach number tests, and with Mach reflection, it is found that the contact surface is not straight, with the angle increasing slightly further away from the reflection point. This may be due to non-uniformity of the inflow as discussed previously for this case (figure 13), or possibly to the influence of the wavelets reflecting off the bottom of the plate holder. Since the transmitted wave angle can be measured much more accurately than the contact surface angle, the angle δ_c determined from the transmitted wave is used in further calculations. The variation of this angle with the wall angle is shown in figure 16 for the coarse test plate, and this plot also indicates a maximum value in the region of transition. However, because of the effect of the wall angle, this does not imply a maximum in the velocity exiting the plate. This latter value is given in figure 17, which shows an approximately continuous increase in exit velocity in the laboratory frame, normal to the plate, as the plate angle increases, combined with increasing velocities as the strength of the incident shock is increased.

In the current tests the aspect ratio of the openings (ratio of width of opening to thickness of plate) is about four times larger than in Friend's (1958) tests. The geometry

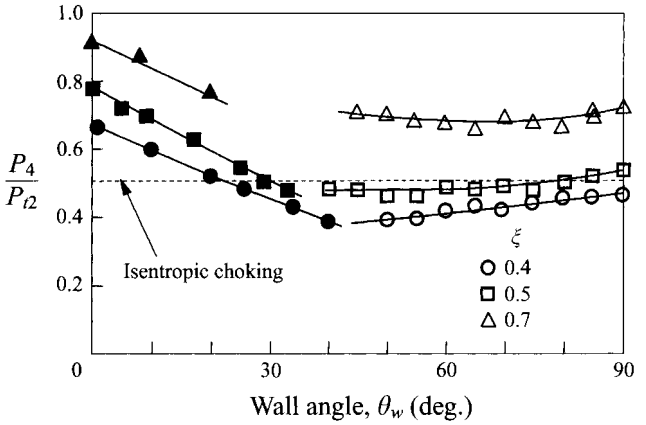

FIGURE 18. The pressure ratio across the plate, normalized to the stagnation pressure above the plate.

of the surface holes will clearly have an effect on the flow through the plate and this would need to be established for a surface made up of randomly distributed pores. For the thin plate that he used Friend assumed that the tangential velocity is conserved across the plate and the agreement he obtained with his experiments tends to support this assumption, whereas in the current tests the experiments show that the flow leaves normal to the surface. The resultant tangential momentum change must thus exhibit itself as a tangential force on the plate. Further measurements will be required to establish the boundary conditions that need to be applied in the more general case of a surface with randomly distributed pores.

The evaluation of the experimental data presented up to this point has resulted in the velocities on either side of the plate being determined. Similar calculations across the shocks also enable the pressures on either side of the plate in regions (ii) and (iv) to be found, and hence the pressure ratios for considerations of choking, and the pressure differences for considerations of flow resistance.

The pressure ratios across the plate (with respect to the stagnation pressure in region (2), in the frame of reference fixed in the plate) are shown in figure 18. Compared to the isentropic choking value of 0.528 it would appear that the flow is choked for the regular reflection results for both the $\xi = 0.4$ and 0.5 cases but not for 0.7. Under Mach reflection conditions the critical pressure ratio is not reached at the smaller wall angles for any of the tests but as the wall angle increases choking can occur. The visual evidence of choking identified in the tests done by Friend (1958), namely the typical oblique-shock diamond pattern of an over- or under-expanded supersonic nozzle, and the existence of a upward-facing auxiliary shock in the downstream flow, are not visible in the current tests, possibly because the slits in the present tests are less than 20% of the width of the openings in Friend's results, and the opening width to plate thickness ratio is four times larger, resulting in the pattern breaking down before emerging into the visible flow region. Based on the sketch of figure 6 the sonic throat of the choked flow will be well into the slit at the position of the vena-contracta of the separated flow.

Friend proposed a simple theory for regular reflection from a perforated plate under choked conditions based on two-dimensional shock theory and the boundary condition that the component of the Mach number normal to the plate (in the steady flow frame of reference) is sufficient to result in sonic flow as determined by the area ratio of the plate. On this basis he defined a discharge coefficient as the ratio of this Mach number

as inferred from the measured shock reflection angle to that calculated from the plate area ratio. It is thus essentially a measure of the vena contracta effect. Discharge coefficients of about 93% were obtained for his tests with strong incident shocks (shock pressure ratios of between 3 and 10). However, for the few tests reported for an incident inverse shock pressure ratio of $\xi = 0.5$, and a 60° wall angle the value had fallen to just less than 70%. Using the same assumptions on the present tests gives coefficients of 0.62 to 0.54 as the wall angle changes from 50° to 80° for $\xi = 0.4$, and about 0.5 for $\xi = 0.5$. This is also similar to the coefficient value of 0.54 determined by Onodera & Takayama (1994) in a slightly different way and using the static pressure in region (ii).

Unfortunately data for vena contracta areas for compressible flows with angled inflows are not available to compare with these data. For an axisymmetric orifice in a pipe the effects of compressibility are dealt with by Ward-Smith (1971) and some of these are pertinent to the present case. For a sharp-edged orifice with separated flow a simple process of choking does not apply since sonic conditions occur at the vena contracta, whose area can change as the boundary conditions change. Thus for fixed upstream conditions, once the flow has choked the vena contracta area increases and moves up towards the inlet for further decreases in back pressure. A similar situation of a range of back pressures for a 'choked' flow is expected to occur in the present case even though separation only occurs on the one wall. The effects of wall thickness to opening size ratio, and of porosity, for incompressible flows have been dealt with by Ward-Smith and although similarities with compressible flows may exist insufficient data are at present available to make meaningful comment. A range of special tests would be required to ascertain the effects of geometry, particularly for the interesting case of randomly distributed pores. In addition theoretical models assume that the porosity is uniformly distributed, and that there is no influence of pore size. The work of Adachi *et al.* (1992) is the strongest indicator that this will only be a reasonable assumption if the incident wave has propagated a distance of about 100 times the pore dimension.

A similar lack of data on loss coefficients makes it difficult to assess the frictional loss through the grid, although from the evidence discussed earlier it appears to be small. Idelchik (1994) is the only work found which treats flow through a grid of rectangular bars with an angled inflow and a perpendicular outflow, thus corresponding to the geometry of the current tests, although it is limited to incompressible flow. The loss is represented as $\zeta = 2\Delta p/\rho w^2 = \sigma_1 \sigma_2$ where w is the downstream velocity, ρ the fluid density, and σ_1 and σ_2 are empirical coefficients, the first of which depends on the inclination of the flow and the second on a combination of the inclination and the openness ratio of the packing. No correlation with the current tests is evident, primarily because his data cover inflow angles up to 60° from the perpendicular only and at that value σ_2 becomes unrealistically large. However, it would appear from the data on transmitted wave strength, and the success of inviscid computational codes, that the reflection and transmitted wave patterns are largely affected by the separation pattern resulting from the shock-wave diffraction into the slit, and the vortex that is developed. Comparing Friend's data with those of the current tests also shows that the length to width ratio of the slit is an important factor, as it is for incompressible flows (Ward-Smith 1971).

6. Conclusion

Detailed characterization of the flow fields following impact of a shock wave on an inclined perforated plate have shown that shock reflected angles are depressed compared to an impervious wall, and the flow into the plate for wall incidences up to about 60° is strongly inclined to the surface, whereafter the angle of flow to the surface steadily increases until it becomes normal to the plate for head-on reflection. The magnitude of the inflow velocity reaches a maximum in the region of transition from regular to Mach reflection, and, in the case of Mach reflection, appears to vary along the plate. The flows in the vicinity of the plate are complex and require further study in order to establish the effects of pore geometry. Treatment of the flow using pseudosteady assumptions appears to be satisfactory, particularly for the case of regular reflection.

The current experimental evidence shows that assumptions made in previous theoretical work are not satisfied. The discrepancies are in two areas. Firstly, it is not uncommon in theoretical approaches to assume that the inflow at the surface of a porous wall is normal to the wall. This assumption is clearly invalid for the present tests, and more work will be required to establish what surface features may influence the inflow. Such tests are under way. Secondly, it is sometimes assumed that the tangential component of momentum is conserved across the surface. Again this is shown not to be true, and in the current tests may be due to the thickness of the plate and the resulting guidance given to the flow as it passes through.

The first author wishes to acknowledge the hospitality of the Institute of Fluid Science of Tohoku University, to express appreciation for the use of the equipment in the Shock Wave Research Center, and for making available the holograms of the Mach reflection tests done in 1986 to complement those done in the present study. In particular, thanks are due to Jiming Yang for assistance in the conduct of the new experiments. Discussions with Dr Hideki Onodera are also gratefully acknowledged.

REFERENCES

ADACHI, T., KOBAYASHI, S. & SUZUKI, T. 1992 An experimental analysis of oblique shock reflection over a two-dimensional multi-guttered wedge. *Fluid Dyn. Res.* **9**, 119–132.

BAER, M. R. 1995 A multiphase model for shock-induced flow in low-density foam. In *Shock Waves@Marseille III, Proc. 19th Intl Symp. on Shock Waves* (ed. R. Brun & L. Z. Dumitrescu), pp. 169–174. Springer.

BEAVERS, G. S. & MATTA, R. K. 1972 Reflection of weak shock waves from permeable materials. *AIAA J.* **10**, 959–961.

BEN-DOR, G., MAZOR, G., TAKAYAMA, K. & IGRA, O. 1987 The influence of surface roughness on the transition from regular to Mach reflection in pseudo-steady flows. *J. Fluid Mech.* **176**, 333–356.

BRAY, R. M. 1984 Reflexion of weak shock waves from acoustically absorbent materials. MSc thesis, College of Aeronautics, Cranfield Institute of Technology.

CLARK, J. F. 1984 The reflection of weak shock waves from absorbent surfaces. *Proc. R. Soc. Lond.* A **396**, 365–382.

CLOUTIER, M., DEVEREUX, F., DOYEN, P. *et al.* 1971 Reflections of weak shock waves from acoustic materials. *J. Acoust. Soc. Am.* **50**, 1393–1396.

DONGEN, M. E. H. VAN, SMEULDERS, D. M. J., KITAMURA, T. & TAKAYAMA, K. 1993 On wave phenomena in permeable foam. *Rep. Inst. Fluid Sci.* **5**, 55–67.

FRIEND, W. H. 1958 The interaction of a plane shock wave with an inclined perforated plate. *UTIA Tech Note* 25. University of Toronto.

GELFAND, B. E., GUBONOV, A. V. & TIMOFEEV. E. J. 1983 Interaction of shock waves in air with a porous screen. *Izv. Akad. Nauk SSSR Mekh. Zhid. Gaza* **4**, 78–84.

GRINTEN, J. G. M. VAN DER, DONGEN, M. E. H. VAN & KOGEL, H. VAN DER 1985 A shock tube technique for studying pore-pressure propagation in a dry and water-saturated porous medium. *J. Appl. Phys.* **58**, 2937–2942.

GUY, T. B. 1973 Attenuation of reflecting shock waves in a duct with absorbent lining. *J. Sound Vib.* **29**, 501–503.

GVOZDEVA, L. G., FARESOV, Y. M., BROSSARD, J. & CHARPENTIER, N. 1986 Normal shock wave reflection on porous compressible materials. In *Dynamics of Explosions* (ed. J. R. Bowen, J. C. Leyer & R. I. Soloukhin). *Progress in Astronautics and Aeronautics*, vol. 106, pp. 155–165.

HORNUNG, H. G. & TAYLOR, J. R. 1982 Transition from regular to Mach reflection of shock waves, Part 1. The effect of viscosity in the pseudosteady case. *J. Fluid Mech.* **123**, 143–153.

IDELCHIK, I. E. 1994 *Handbook of Hydraulic Resistance*. Boca Raton: CRC Press.

KOBAYASHI, S., ADACHI, T. & SUZUKI, T. 1995 Regular reflection of a shock wave over a porous layer: theory and experiment. In *Shock Waves@Marseille IV, Proc. 19th Intl Symp. on Shock Waves* (ed. R. Brun & L. Z. Dumitrescu), pp. 175–180. Springer.

LEVY, A., BEN-DOR, G., SKEWS, B. W. & SOREK, S. 1993 Head-on collision of normal shock waves with rigid porous materials. *Exps. Fluids* **15**, 183–190.

LI, H., LEVY, A. & BEN-DOR, G. 1995 Analytical prediction of regular reflection over porous surfaces and comparisons with experiments. *J. Fluid Mech.* **282**, 219–232.

NEUMANN, J. VON 1943 Oblique reflection of shocks. *Explos. Res. Rep.* 12. Dep. Navy, Washington D.C. Also in: *Collected works*, vol. 6, pp. 238–99, Pergamon (1963).

ONODERA, H. & TAKAYAMA, K. 1990*a* Shock wave propagation over slitted wedges. *Rep. Inst. Fluid Sci.* **1**, 45–66.

ONODERA, H. & TAKAYAMA, K. 1990*b* Interaction of a plane shock wave with slitted wedges. *Exps. Fluids* **10**, 109–115.

ONODERA, H. & TAKAYAMA, K. 1994 Analysis of shock wave propagation over perforated wall and its discharge coefficient. *JSME Intl J.* B, 37, 497–502.

REICHENBACH, H. 1985 Roughness and heated layer effects on shock wave propagation and reflection – Experimental results. *Ernst Mach Institut Rep* E25/85.

SKEWS, B. W. 1967*a* The shape of a diffracting shock wave. *J. Fluid Mech.* **29**, 297–304.

SKEWS, B. W. 1967*b* The perturbed region behind a diffracting shock wave. *J. Fluid Mech.* **29**, 705–719.

SKEWS, B. W. 1971 An experimental study of the interaction of shock waves with bends in a duct. *Symp. on Internal Flows, University of Salford* (ed. J. L. Livesey), pp. D41–D45. Dept Mech. Engng, Salford University.

SKEWS, B. W. 1991 The reflected pressure field in the interaction of weak shock waves with a compressible foam. *Shock Waves* **1**, 205–211.

SKEWS, B. W. 1994 Oblique reflection of shock waves from rigid porous materials. *Shock Waves* **4**, 145–154.

SKEWS, B. W. 1995 Shock wave impact on porous materials. In *Shock Waves@Marseille III, Proc. 19th Intl Symp. on Shock Waves* (ed. R. Brun & L. Z. Dumitrescu), pp. 11–20. Springer.

SMITH, L. G. 1945 Photographic investigation of the reflection of plate shocks in air. *OSRD Rep.* 6271.

SUZUKI, T. & ADACHI, T. 1987 Comparison of shock reflections from a dust layer with those from a smooth surface. *Theor. Appl. Mech.* **35**, 345–352.

TAKAYAMA, K. 1983 Application of holographic interferometry to shock wave research. *Proc. SPIE* **398**, 174–180.

TAKAYAMA, K., ONODERA, O. & GOTAH, J. 1882 Shock wave reflection over a wedge with surface roughness or curved surface (in Japanese). *Rep. Inst. High Speed Mech. Tohoku University*, vol. 48, pp. 1–21.

WARD-SMITH, A. J. 1971 *Pressure Losses in Ducted Flows*. Butterworths.

YANG, J.-M., ONODERA, O. & TAKAYAMA, K. 1994 Characteristics of a diaphragmless shock tube for generating weak shock waves by using a quickly moving rubber membrane. *Trans. Japan Soc. Mech. Engrs* B **60**, 473–479.